

# Thermochromic liquid crystals applied for heat transfer research

J.A. STASIEK\*<sup>1</sup> and T.A. KOWALEWSKI<sup>2</sup>

<sup>1</sup>Faculty of Mechanical Engineering, Technical University of Gdańsk, 11/12 Narutowicza Str.,  
80-952 Gdańsk, Poland

<sup>2</sup>Institute of Fundamental Technological Research, Polish Academy of Sciences, 21 Świątokrzyska Str.,  
00-049 Warsaw, Poland

---

---

*In recent years thermochromic liquid crystals (TLC) have been successfully used in non-intrusive heat transfer and fluid mechanics studies. Thin coatings of TLC's at surfaces are utilised to obtain detailed heat transfer data of steady or transient process. Application of TLC tracers allows instantaneous measurement of temperature and velocity fields for two-dimensional cross-section of flow. Computerised flow visualisation techniques allow automatic quantification of temperature of the analysed surface or the visualised flow cross-section. Here, we describe our experience in applying the method to selected problems studied in our laboratory. They include modelling of flow configurations in the differentially heated inclined cavity with vertical temperature gradient simulating up-slope flow as well as thermal convection under freezing surface. The main aim of these experimental models is to generate reliable experimental database on velocity and temperature fields for specific flow. The methods are based on computerised true-colour analysis of digital images for temperature measurements and modified particle image velocimetry and thermometry (PIVT) used to obtain the flow field velocity.*

---

---

**Keywords:** temperature measurements, liquid crystals thermography, particle image velocimetry and thermometry.

## 1. Introduction

Liquid crystals are highly anisotropic fluids that exist between the boundaries of the solid phase and the conventional, isotropic liquid phase. The TLC based temperature visualisation is based on the property of some cholesteric and chiral-nematic liquid crystal materials to reflect definite colours at specific temperatures and viewing angle. The colour change for the TLC ranges from clear at ambient temperature, through red as temperature increases and then to yellow, green, blue and violet before turning colourless (isotropic) again at a higher temperature. They appear colourless above and below the active range. The colour-temperature play interval depends on the TLC composition. It can be selected for the bands of about 0.5°C to 20°C, and working temperature of –30°C to above 120°C. These colour changes are repeatable and reversible as long as the TLC's are not physically or chemically damaged. The response time of TLC's equals about 10 ms. It is short enough for typical thermal problems in fluids. Since the colour change is reversible and repeatable, they can be calibrated accurately with a proper care and used in this way as temperature indicators. They can be painted on a surface or suspended in a fluid and used to indicate visibly the temperature distribution. Thus, liquid crystals have been successfully applied to heat transfer and fluid flow research.

During the past, liquid crystals have been extensively applied to the qualitative visualisation of entire steady state, or transient temperature fields on solid surfaces. Since quantifying colour is difficult and somewhat ambiguous task, application of thermochromic liquid crystals initially was largely qualitative. Application of the colour films or interference filters was tedious and inaccurate. First application of true-colour digital image processing gave impact to qualitative and fast temperature measurements. Rapid development of the hardware and software computerised image processing techniques made possible now to set-up inexpensive system capable for real-time transient full-field temperature measurements using TLCs. In this paper, we review the above issues and use illustrative examples from our own work in applying TLC to the study of forced and natural convective heat transfer on a cooled surface heated by air flow disturbed by a number of complex geometrical configurations and for temperature and flow visualisation in closed cavities also with phase change. Significance of the full-field temperature and flow measurements for verification of numerical results becomes evident. We found that only with help of the full-field measurements it was possible to identify serious discrepancies between numerical predictions and the experimental observations. With the help of experimental feedback, it was possible to introduce necessary modifications to numerical codes and in such a way to improve its output in the correct direction.

\* e-mail: jstasiek@pg.gda.pl

## 2. Liquid crystals thermography

Liquid crystals are temperature indicators that modify incident white light and display colour whose wavelength is proportional to temperature. They can be painted on a surface or suspended in the fluid and used to make visible the distribution of temperature. Normally clear, or slightly milky in appearance, liquid crystals change in appearance over a narrow range of temperature called the “colour-play interval” (the temperature interval between first red and last blue reflection), centred around the nominal “event temperature.” The displayed colour is red at the low temperature margin of the colour-play interval and blue at the high end (Fig.1). Within the colour-play interval, the colours change smoothly from red to blue as a function of temperature. Pure liquid crystal materials are thick, viscous liquids, greasy and difficult to deal with under most heat transfer laboratory conditions. The TLC material is also sensitive to mechanical stress. A micro-encapsulation process which encloses small portions of liquid crystal material in polymeric material was introduced to solve problems with the stress sensitivity as well as with the chemical deterioration. For surface temperature measurements application of the unencapsulated material (unsealed liquids) to a clear plastic sheet and sealing it with a black backing coat to form a pre-packaged assembly is used. Commercially available temperature indicating devices using TLC contain a thin film of the liquid crystal sandwiched be-

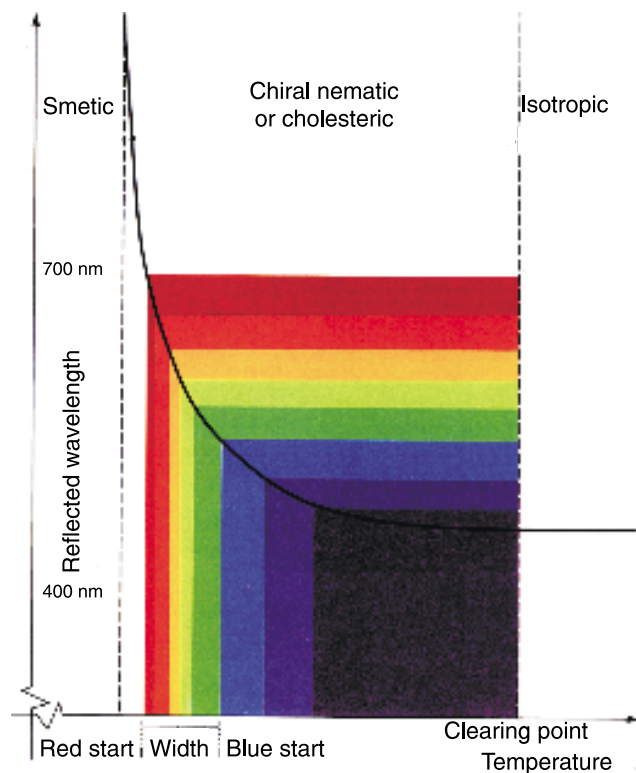


Fig. 1. Typical reflected wavelength (colour) temperature response of a TLC mixture.

tween a transparent polyester sheet and a black absorbing background, however in the current experiment the liquid crystals are deposited on the black painted sheet. For flow analysis the suspension of thermochromic liquid crystals can be used to make visible the temperature and velocity fields in liquids. By dispersing the liquid crystal material into the liquid they become not only classical tracers used for flow visualisation but simultaneously small thermometers monitoring local fluid temperature [1–5]. The collimated source of white light must be used to illuminate selected cross-section of the flow (light sheet technique) and colour images are acquired at perpendicular direction.

In the following examples the unencapsulated TLC’s tracers have been applied to measure both temperature and velocity flow fields. We found that light scattered by the capsule shell inevitable diminishes saturation of the observed colours. Because the stress effects are negligible for slow motion we prefer application of fine dispersed raw material in flow measurements.

### 2.1. Surface temperature measurements

Before the execution of a thermal or flow visualisation experiment, we should recognise the characteristics of overall combination of the TLC, light source, optical and camera system, and make a rational plan for total measurement

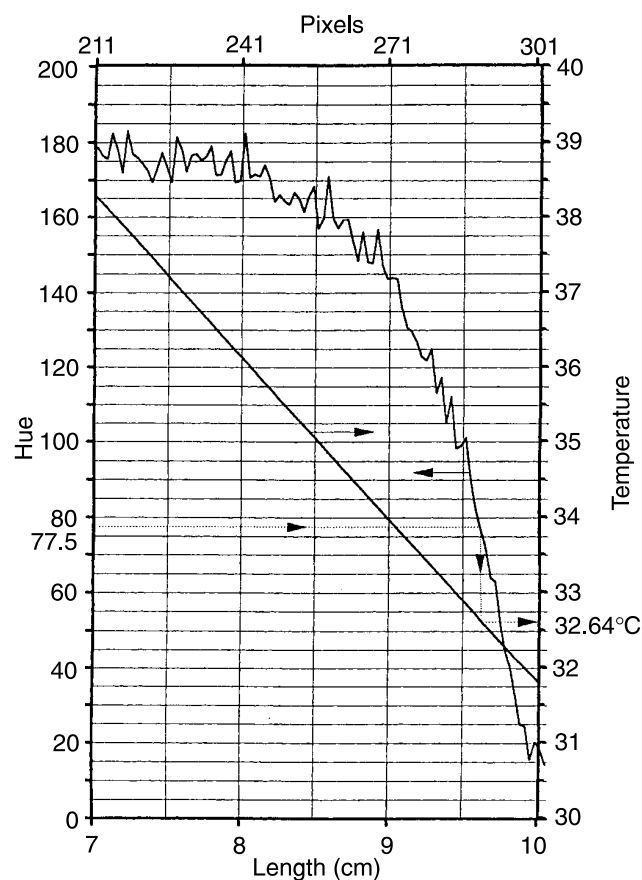


Fig. 2. Representative calibration curve – Hue and temperature distribution along the test plate.

system. The relationship between the temperature of the crystal and the measured Hue of the reflected light defines the calibration curve for the liquid crystal. The result is a curve relating the Hue of the reflected light to the surface temperature. A known temperature distribution exists on a "calibration plate" (brass plate) to which is attached the liquid crystal layer. In order to maintain a linear temperature distribution with desired temperature gradients, one end of a brass plate was cooled by stabilised water and the other end controlled electrically to give a constant temperature [6]. The brass plate with the liquid crystal layer is calibrated in place in the wind tunnel with the same lighting level and viewing angle used during the data acquisition phase of the experiment. The distribution of the colour component pattern on the liquid crystal layer was measured by RGB colour camera and a series of images at different temperatures defines the calibration.

A representative calibration curve including Hue and temperature distribution along the plate is shown in Fig. 2. The liquid crystals used here, manufactured in sheet form by B&H Limited [7] (Fig. 3), had an event temperature range of 30.7–33.3°C. In the actual measurements, only the yellow-green colour band corresponding to  $t_1 = 32.1^\circ\text{C}$  was used as it is the brightest and sharpest. In this particular experiment uncertainty was estimated as about  $0.05^\circ\text{C}$  by

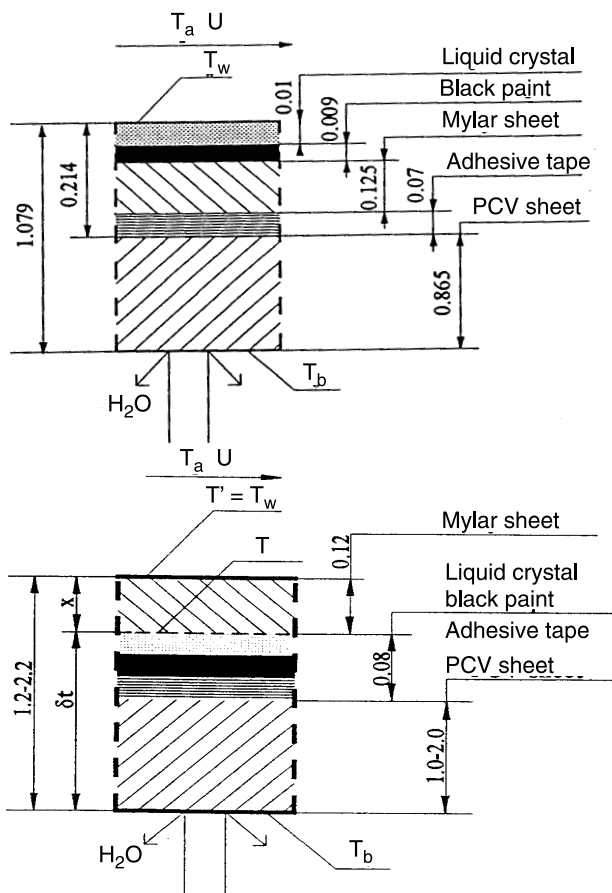


Fig. 3. Liquid crystal package (front print and waterproof).

considering only the section of the surface used in the experiment, span wise non-uniformities in Hue value are minimised. For the surface temperature measurement HIS colour image processing is utilised. These include image transformations, enhancement, analysis, compression, transformation and restorations. Building on grey-scale image processing hardware and software, Data Translation [8] has produced a  $512 \times 512$  pixels  $\times 8$  bit per colour component colour frame-grabber board for PC/ATs which takes up a 256 K byte of memory. The two dimensional temperature distribution is determined using RGB video-camera, IBM 386 Personal Computer AT, HSI Colour Frame Grabber DT 2871 and Auxiliary Frame Processor DT 2858. As it is shown, the chart is also for an RGB video-recorder (JVC-S605E), includes a Time Based Corrector VT 3000 and KMV7EK RGB converter. New chart with JVC-S605E as the terminal makes it possible for presentation tapes to be loaded, cued and played exactly on a schedule with all operations handed by the computer. For fast and transit method, accurate location of specific scenes or edit points JVC-S605E is provided with a convenient and easy-to-use search dial. A time base corrector (TBC) controls times tracking systems and easy identification colour-coded images.

Two main methods of surface temperature measurement are performed involving steady state and transient techniques. A brief history of these is given by Baughn *et al.* [9]. Recent reviews of heat transfer measurements have been also produced by Akimo [6], Moffat [10,11], Jones *et al.* [12], Ashforth-Frost *et al.* [13], and Stasiek [14].

### 2.1.1. Steady state analyses – constant flux method

The steady state techniques employ a heated model and the TLC is used to monitor the surface temperature. Usually, a surface electric heater is employed such that the local flux,  $q$  is known and this, together with the local surface temperature,  $T_w$ , (found from the TLC), gives the local heat transfer coefficient,  $h$

$$q = I^2 r \quad \text{and} \quad h = \frac{q}{T_a - T_w}. \quad (1)$$

$T_a$  is a convenient driving gas temperature,  $I$  is the current and  $r$  is the electrical resistance per square of the heater.

### 2.1.2. Steady state analyses – uniform temperature method

The TLC-coated test specimen forms one side of a constant temperature water bath and is exposed to a cool/hot air flow. The resulting thermograph is recorded on film or video and further measurement positions are obtained by adjusting the water bath temperature. This method is more time consuming due to the large volume of water that needs to be heated. In this case, the heat transfer coefficient

is determined by equating convection to the conduction at the surface

$$h(T_a - T_w) = \frac{k}{x}(T_w - T_b), \quad (2)$$

where,  $T_b$  is a water-side temperature of the wall,  $x$  the wall thickness, and  $k$  the thermal conductivity.

### 2.1.3. Transient method

This technique requires measurement of the elapsed time to increase the surface temperature of the TLC-coated test specimen from a known initial temperature predetermined value. The rate of heating is recorded by monitoring the colour change patterns of the TLC with respect to time. If the specimen is made from a material of low thermal diffusivity and chosen to be sufficiently thick, then the heat transfer process can be considered to be one-dimensional (1-D) in a semi-infinite block. Numerical and analytical techniques can be used to solve the 1-D transient conduction equation. The relationship between wall surface temperature,  $T$ , and heat transfer coefficient,  $h$ , for the semi-infinite case is

$$\frac{T - T_i}{T_a - T_i} = 1 - e^{\beta^2} \operatorname{erfc}(\beta); \quad \beta = h \left( \frac{t}{\rho c k} \right)^{0.5} \quad (3)$$

where,  $\rho$ ,  $c$  and  $k$  are the model density, specific heat and thermal conductivity.  $T_i$  and  $T_a$  are the initial wall and gas temperatures and  $t$  is time from initiation of the flow, Baughn *et al.* [9] and Jones *et al.* [12]. More recently Leiner *et al.* [15] developed a new formula for evaluation of heat transfer coefficient  $h$  in the following form

$$h = -\frac{\delta \rho c}{t} \ln \left[ \frac{T_a - T}{T_a - T_i} \right] \quad (4)$$

where,  $\delta$  is the plate wall thickness and the transit local surface temperature  $T$  is detected after a time interval  $t$ .

## 2.2. Full-field temperature and velocity measurements

The temperature visualisation is based on the property of some cholesteric and chiral-nematic liquid crystal materials to refract light of selected wavelength as a function of the temperature and viewing angle. The response time of TLCs equals about 3 ms. It is short enough for typical thermal problems in fluids. In the experimental realisation, the investigated flow has to be illuminated by a light sheet. The arrangement is similar to that used for classical PIV experiments, however, white light is necessary to obtain selected colour refraction from the TLC particles. The colour of light refracted by TLCs depends not only on temperature

but also on the observation angle. Therefore, it is important that the investigated flow is illuminated by well-defined light plane and observed by a camera from a fixed direction. Density of the TLC material is very closed to that of water and in most cases the TLC tracers can be treated as neutrally buoyant. Figure 4 demonstrates application of unencapsulated TLC tracers for visualisation of natural convection in a differentially heated cube-shaped cavity. The hue (chromaticity) represents the dominant wavelength of the colour, i.e., the value that depends directly on the TLCs temperature. The temperature is determined by relating the hue to a temperature calibration function. The 8-bit representation of the hue value assures resolution better than 1%. However, the colour-temperature relationship is strongly non-linear (comp. Fig. 5). Hence, the accuracy of the measured temperature depends on the colour (hue) value, and varies from 3% to 10% of the full colour play range. For the liquid crystals typically used it results in the absolute accuracy of 0.15°C for lower temperatures (red-green colour range) and 0.5°C for higher temperatures (blue colour range). The most sensitive region is the colour transition from red to green and takes place for a temperature variation less than one Celsius degree. The 2-D velocity vector distribution has been measured by digital particle image velocimetry. By this method, the motion of the scattering particles, observed in the plane of the illuminating light sheet, is analysed. For this purpose, the colour images of the TLC tracers are transformed to black and white intensity images. To improve contrast and particles visibility a special filtering technique is applied. It allows obtaining bright images of the tracers, well suited for PIV. The

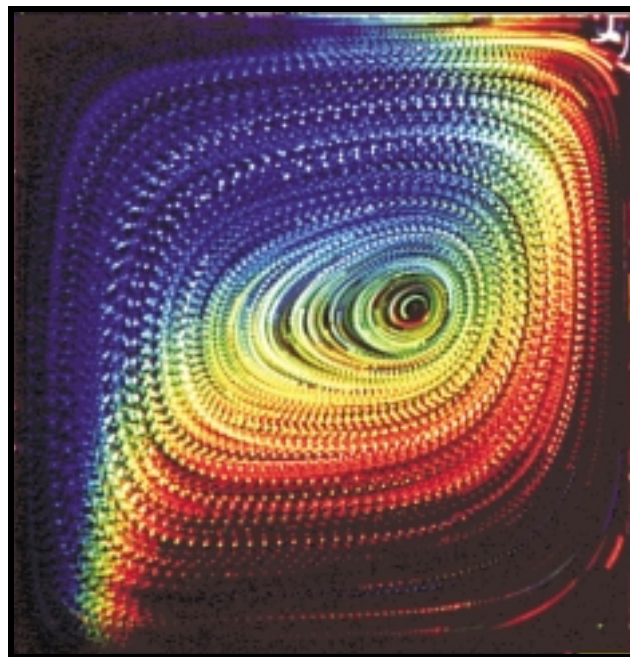


Fig. 4. Multiexposed colour photograph of the convective flow seeded with liquid crystal tracers. Tracers change colour from blue to red following the clock-wise flow circulation from the hot wall (left side) to the cold wall (right side).



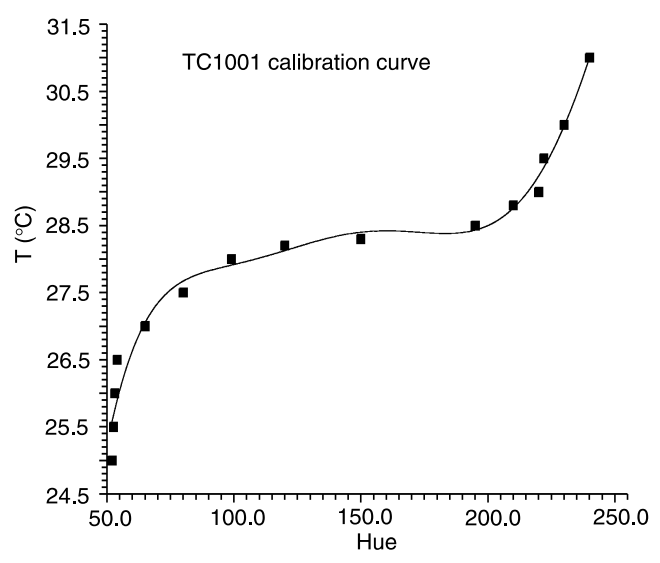


Fig. 5. Temperature vs. hue for TLCs sample used to study natural convection of water. Calibration curve obtained by the 6<sup>th</sup> order polynomial fitted to the experimental points.

cross-correlation analysis performed between different images of the sequence (time interval between pairs changes) allows us to preserve similar accuracy for both the low and high velocity flow regions. For typical displacement vector of 10 pixels the relative accuracy of the velocity measurement (for single point) is better than 6%. The typical experimental setup used for the flow measurements [1,2] consists of a convection box, a halogen tube lamp, the 3-chip CCD colour camera and the 32-bit frame grabber. The flow field is illuminated with a 2-mm thin sheet of white light from a specially constructed halogen lamp or xenon-flash tube and observed in the perpendicular direction. The 24-bit colour images, typically of 768x564 pixels, have been acquired with a personal computer. Using PCI based colour frame grabber (AM-STD ITI) and a 128MB Pentium computer, our setup permits us to gain in real time over 50 RGB images, before they have to be saved on the computer magnetic disk.

### 3. Application experiments

In order to demonstrate feasibility of TLC techniques in practical heat transfer contexts, the authors have performed several experiments (Figs. 6 and 7). The first set was carried out to investigate temperature and heat transfer coefficient distributions on a cooled surface heated by an air flow and disturbed by a number of complex geometrical configurations, namely:

- square roughness elements and rib-roughened channel,
- crossed-corrugated and corrugated-undulated elements as used in rotary heat exchangers (regenerators),
- flat plate heat exchanger element and impinging jet.

In the second set of experiments, the flow velocity and temperature distribution in a small cavities were observed.

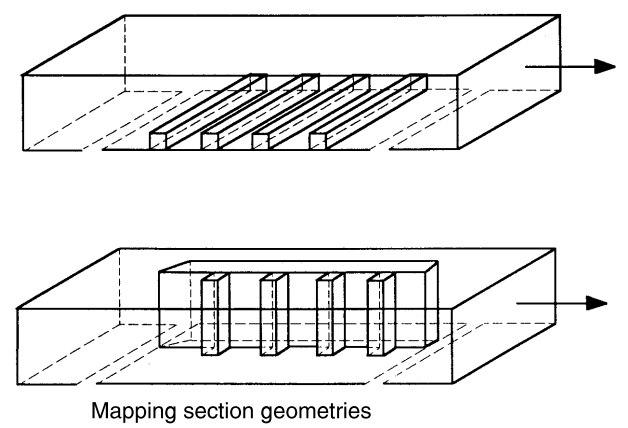


Fig. 6. Mapping section geometries with square roughness elements and rib-roughened channel.

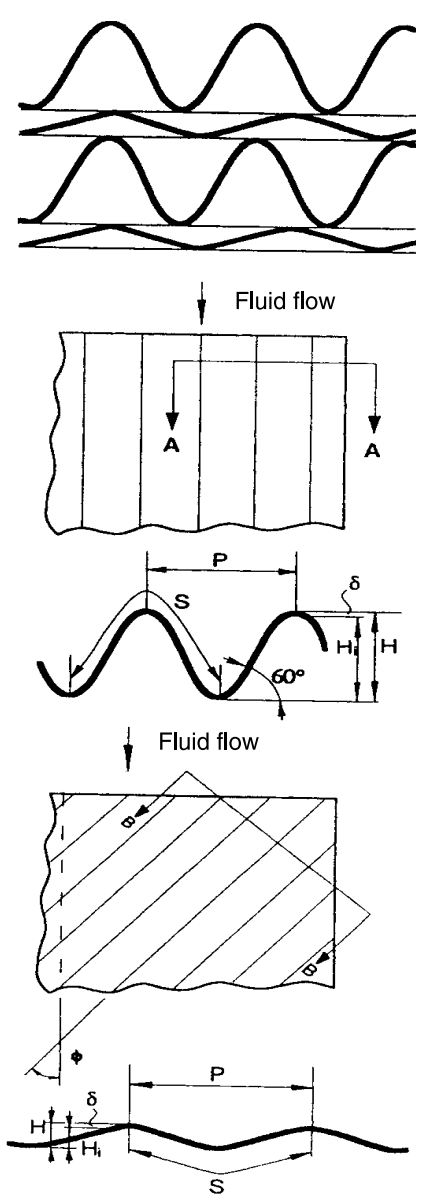
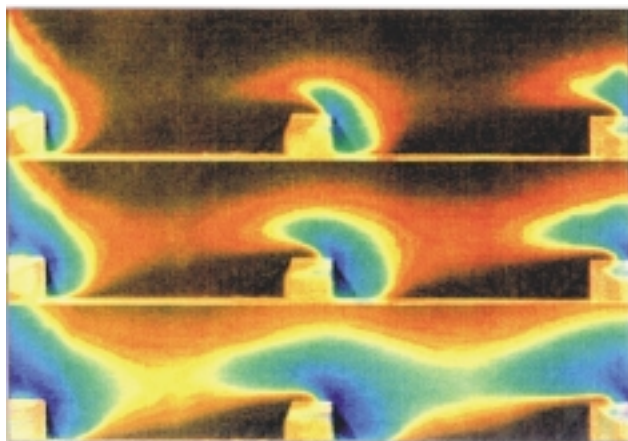


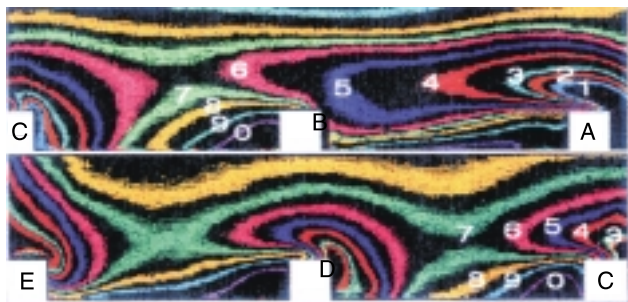
Fig. 7. Working section – general view of corrugated-undulated heat transfer element.

### 3.1. Surface temperature measurements – selected results

The experimental study was carried out using an open low-speed wind tunnel consisting of entrance section with fan and heaters, large settling chambers with diffusing screen and honeycomb, and then mapping and working sections. Air is drawn through the tunnel using a fan able to give Reynolds numbers of between 500 and 50,000 in the mapping and working sections. The working air temperature in the rig range between 25°C to 65°C produced by the heater positioned just down stream of the inlet. The major construction material of the wind tunnel is perspex. Local and mean velocity are measured using conventional Pitot tubes and DISA hot-wires velocity probe. The alternative effects of constant wall temperature and constant heat flux boundary conditions are obtained using a water bath, while the temperature is controlled with a thermostat capable of establishing and maintaining temperature to within 0.01°C accuracy. Photographs are taken using a RGB video-camera and true-colour image processing system. The heat transfer coefficient is a defined quantity, calculated from the surface heat flux and the difference between the surface temperature and some agreed reference temperature.



(a)



(b)

Fig. 8. True-colour images from liquid crystal thermography for an endwall surface with in-line square ribs (left) (a); pattern of ten Nusselt number  $Nu$  reconstructed by false colour images of the heat transfer surface for  $Re = 20000$  (No. 0:  $Nu = 79$ ; 9: 99; 8: 113; 7: 123; 6: 136; 5: 147; 4: 160; 3: 175; 2: 185; 1: 209) (b).

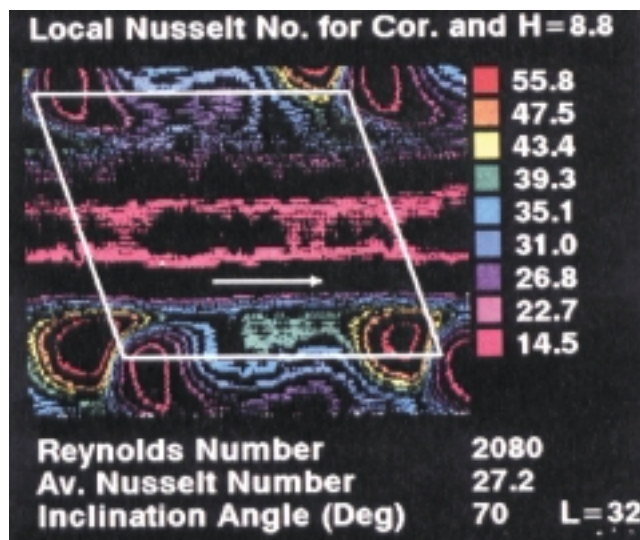


Fig. 9. False colour image of local Nusselt number contours over a central diamond of the undulated plate of corrugated-undulated geometry ( $\alpha = 70^\circ$ ,  $Re = 2080$ ,  $H = 8.8$  mm,  $L = 32$  mm).

This is usually the far field temperature, the mixed mean temperature or the adiabatic surface temperature. Liquid crystals can be used to determine the distribution of the surface temperature, and if the surface heat flux can be found, this allows evaluation of the heat transfer coefficient or the Nusselt number. The alternative effects of constant wall temperature and constant heat flux boundary conditions are obtained using a water bath. Photographs are taken using a RGB video-camera and a true-colour image processing technique. Usually several isotherms (each corresponding to a different heat flux) are taken by RGB video-camera to record the local Nusselt contours under an oblique Reynolds number. The locations of each isotherm and colour (adjusted to each Nusselt number) are digitised following a projection of the false colour image on a digitising image respectively (this particular method can be called “image combination technique” ICT). Figure 8(a) shows photographs of the colour distribution of the liquid crystal layer around square section column, image of the computer display after segmentation processing (Hue: 45-55) and false colour image processing (ICT) respectively on bottom. Also (as mentioned above) liquid crystal thermography has been applied to the study of heat transfer by forced convection from a square roughness elements. A sample of the results for these studies is shown in Fig. 8(b). Recording the colour pattern by a RGB video-camera and converting the stored image to the HSI domain allows one to reconstruct the isotherm lines in the new colour scale (ICT) selected arbitrarily for better understanding and visualisation of heat transfer and fluid motion. Also Fig. 9 shows a false colour image of local Nusselt number contours over a central diamond of the corrugated-undulated heat exchanger surfaces. The cross corrugated and corrugated-undulated surfaces are frequently employed to increase heat transfer coefficient for high heat flux applica-

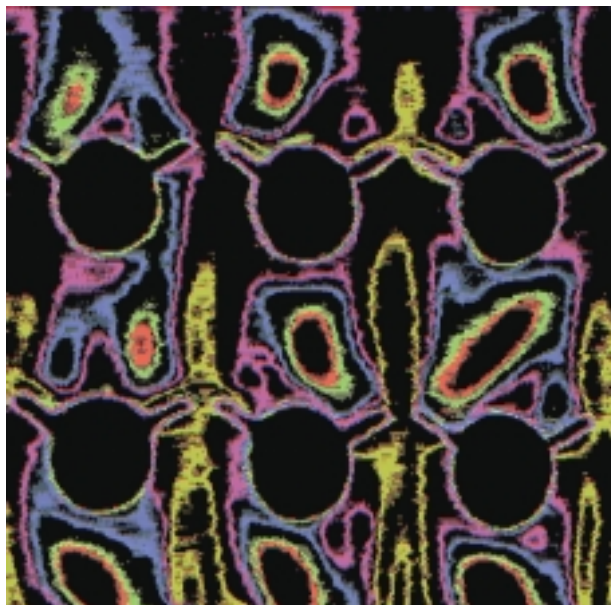


Fig. 10. False colour image of local Nusselt number contours. Local Nusselt number: red – 6.80, green – 7.82, blue – 11.98, violet – 14.60, khaki – 22.15 ( $Re = 1690$ ; Average Nusselt number – 14.5).

tions (Fig 9). Improvement in their flow and thermal characteristics does not require any demonstrations and would substantially reduce fuel and production costs. The measuring technique comprising the use of LC flexible sheets and true-colour processing may also be used for a great variety of applications and should be of considerable use in improving the design of all types of compact heat exchanger. Experimental procedure cover full-field flow patterns in classic heat exchanger elements (flat plate with fine-tubes in-line, staggered and with vortex generators) describing local heat transfer coefficient and Nusselt number on the surfaces. Example of such results is presented in Fig. 10. Impinging jets associated with water jet, air-water spray

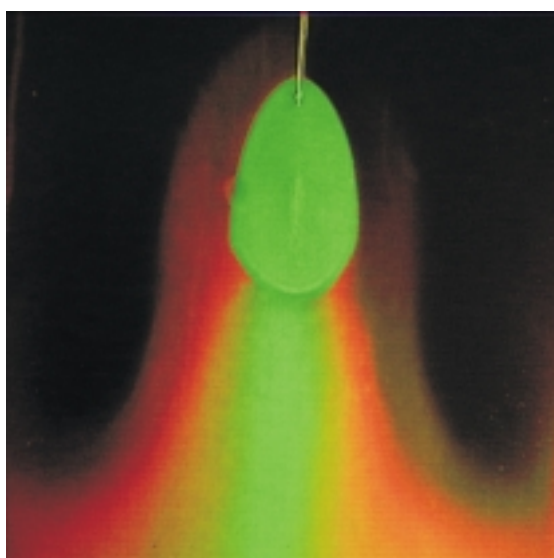


Fig. 11. True-colour image of water impinging jet on a liquid crystal coated surface.

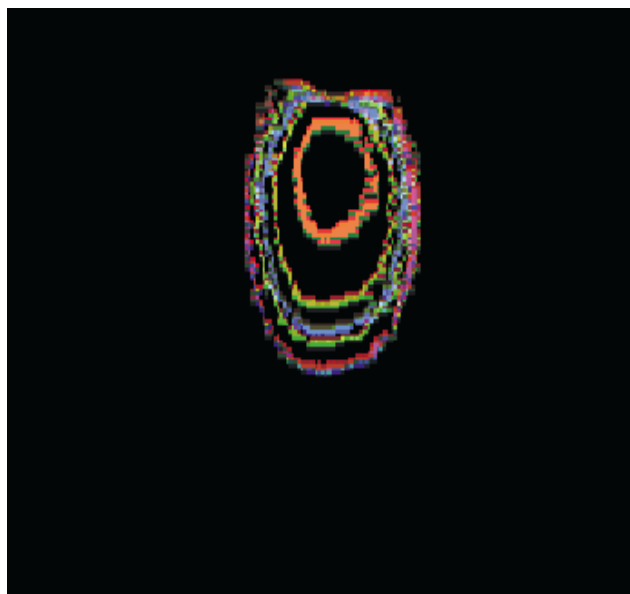


Fig. 12. False colour image of local Nusselt number contours. Local Nusselt number: red – 39.2, khaki – 14.9, blue – 11, green – 9.1, violet – 5.98 (Average Nusselt number – 15.03).

and air jet are widely used to provide high local heat and/or mass transfer in a various of applications including metal rolling processes, glass manufacturing, paper drying or gas turbine cooling. They offer the potential of high heat transfer rate and relative ease of controlling specific areas to be cooled (heated, dried, or moisten). In order to study the influence of thermo-mechanical properties and geometry of an oblique impinging jet on heating or cooling practices on/from plate, a good understanding of the heat add mass aspects of the process is essential (Figs. 11 and 12).

### 3.2. Natural convection in a closed cavity – selected results

Vertical temperature gradients are mainly responsible for the atmospheric or oceanographic fluid motion. Development of the nocturnal stable stratification over flat areas,

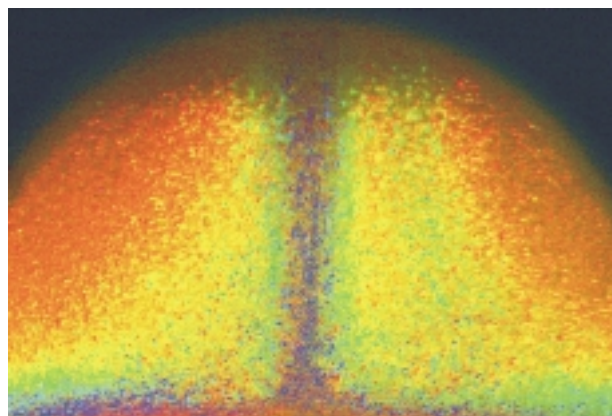


Fig. 13. TLCs visualisation of a thermal aloft generated over locally heated bottom wall of a water basin.



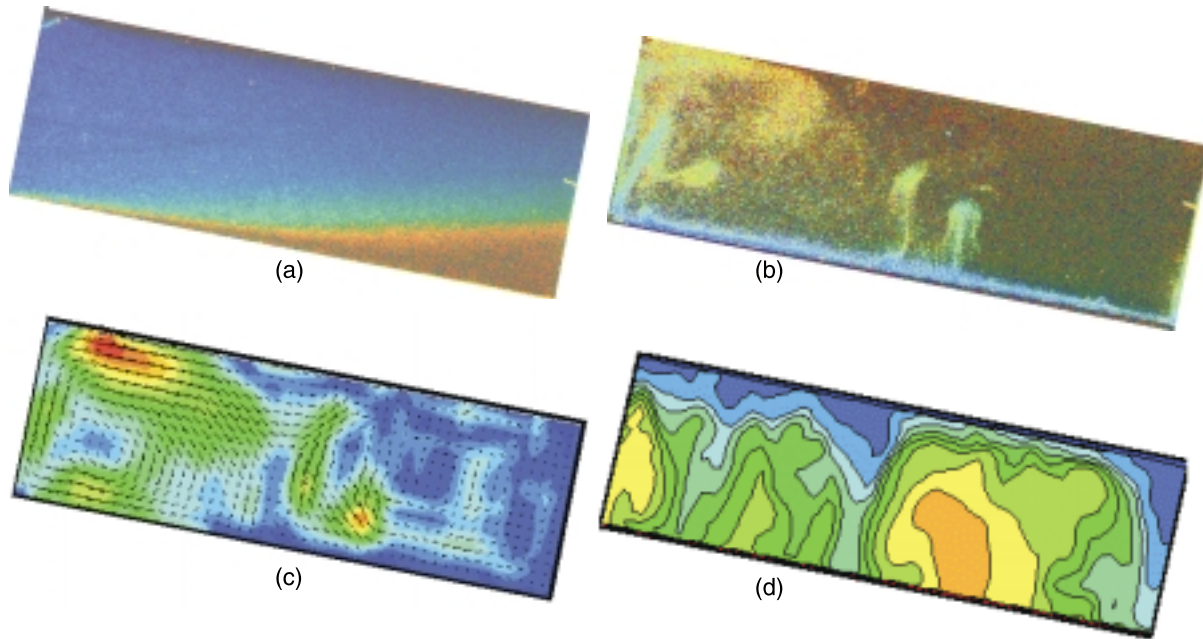


Fig. 14. Convection observed for water in the tilted channel with 11°C temperature difference between top and bottom wall. TLCs visualisation of temperature field for stable thermal stratification (a), visualisation of temperature field with convective instabilities for negative temperature gradient (b), PIV evaluated velocity field with velocity magnitude contours (c), temperature field in the numerical simulation (d).

inversion of temperature gradient and breakup of the convective boundary layer developed at the ground levels can be simulated using small-scale laboratory experiments. One of the typical features characterising instabilities generated by vertical temperature gradient are plums or ejections appearing, when the thermal boundary layer breaks up. Figure 13 shows visualisation of the thermal jets generated by local heating of the flat surface. The hot liquid accelerates creating “a micro tornado” above the surface. Using liquid crystals suspension this fluid motion can be well quantified in terms of temperature and velocity fields.

Similar flow structures, appearing in a quasi-periodic sequence are observed in the experiment simulating transition from stable to unstable thermal stratification. A rectangular cavity with isothermal top and bottom wall is used to

generate the flow. For fully horizontal orientation flow pattern in such geometry is well known as Rayleigh-Bénard type, with characteristic instability arising for negative temperature gradients. Tilting the cavity generates additional convective motion commences along the walls, similarly to up or down slope motion in the atmosphere. Figure 14(a) shows stable stratified configuration with cold bottom and warm fluid above, typical for nocturnal configuration of the atmosphere. Destabilising effects of forced convection (low winds) can be visualised by imposing external flow field. By reversing temperature gradient (diurnal configuration) the convective boundary layer starts to move pushing fluid up the slope [Figs. 14(b), (c) and (d)]. The flow induces instabilities breaking the thermal boundary layer and producing quasi-periodic vertical ejections of

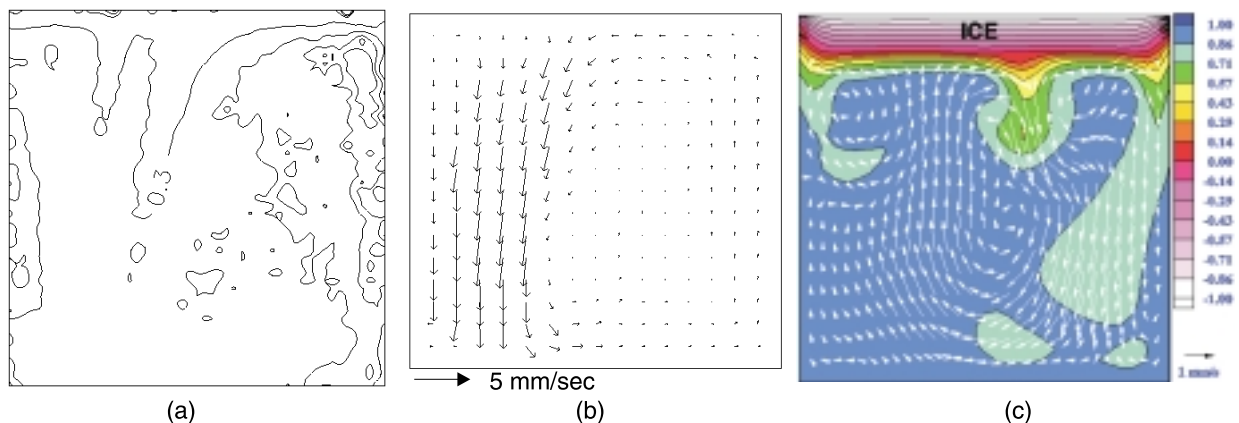


Fig. 15. Typical instabilities measured during the onset of convection: temperature (a) and velocity (b) fields at the centre plane of the cube shaped cavity;  $T_h = 21^\circ\text{C}$ ,  $T_c = 15^\circ\text{C}$ ,  $Ra = 2.7 \times 10^6$ ,  $Pr = 8$ ; (c) – numerical simulations (h – hot wall, c – cool wall).



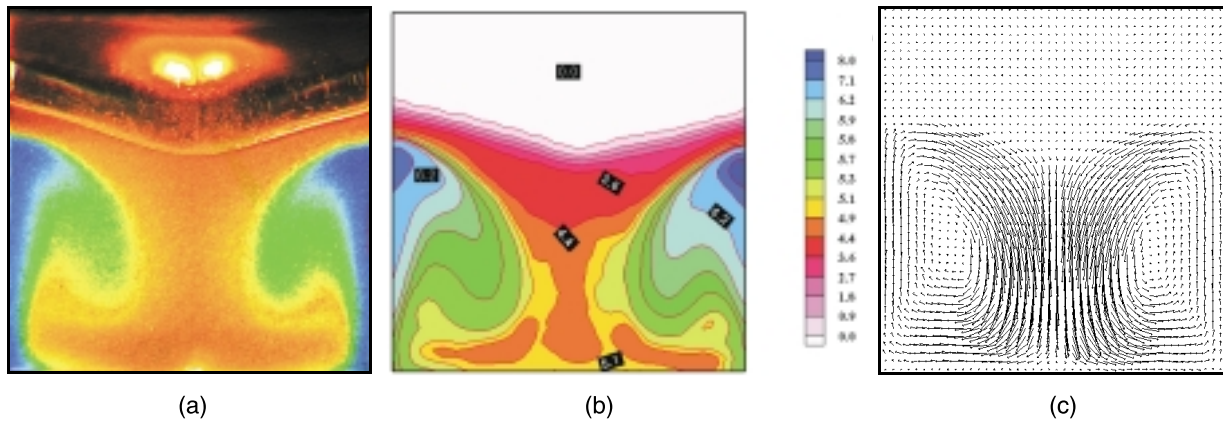


Fig. 16. Freezing of water under cold surface in lid cooled cavity. Recorded image of TLC tracers (a), evaluated temperature (b) and velocity (c) fields. Time step – 3600 s after cooling starts; Isothermal lid temperature  $T_c = -10^\circ\text{C}$ , external temperature  $T = 20^\circ\text{C}$ .

warmer fluid, and similar cold fluid plums falling down from the top wall. This type of instability depends on the slope inclination and thermal parameters and is primary agents responsible for the vertical mixing processes in the convective boundary layer. Both velocity the measured temperature and velocity fields indicate presence of thermal up draughts and downdraughts. Numerical simulation performed using commercial code Fluent shows main features of the experiment [Fig. 14(d)].

Generation of the thermal instabilities can be well observed in the experiment with cooling from the top in a cube shaped cavity. The top wall of the cavity is isothermal at low temperature and the other five walls are non-adiabatic, allowing a heat flux from the fluid surrounding the box. This configuration was used to study natural convection of water without and with phase change [2,3] (freezing from the top). Physically this configuration resembles the Rayleigh-Bénard problem. However, due to non-adiabatic boundary conditions at the sidewalls, the flow structure is different. For the cube shaped cavity symmetry of the enclosure imposes a strong downward flow along the vertical axis of symmetry. However, before a stable final flow structure is achieved, several oscillatory changes in its pattern are observed. The initial flow instabilities can be well seen in temperature and velocity fields visualised in the box [Figs. 15(a) and (b)]. Numerical simulations confirmed that onset of convection is followed by formation of several cold thermals responsible for strong mixing in the box [Fig. 15(c)].

The formation of ice has been studied by decreasing the lid temperature down to  $-10^\circ\text{C}$ . A complicated flow pattern, which establishes, becomes visible also in the structure of the ice surface. It was found that the creation of the ice layer at the lid has a stabilising effect on the flow. Figure 16 shows the temperature and velocity field evaluated at the time step 3600 s for this case. It appears that even this quasi-steady result is only qualitatively well described by numerical model. One of the possible reasons is strong sensitivity of this configuration to imposed thermal boundary conditions at the sidewalls.

## 4. Conclusions

A new experimental technique, in this case true-colour image processing of liquid crystal patterns, allows new approaches to old problems and at the same time opens up new areas of research. Image processed data makes available quantitative, full-field information about the distribution of temperature and heat transfer coefficient which will undoubtedly encourage the study of situations which have been, until now, too complex to consider. The measuring technique comprising the use of LC flexible sheets and true-colour processing may also be used for a great variety of applications and should be of considerable use in improving the design of all types of rotary and compact heat exchanger. Also computer-aided analysis of colour images of unsealed TLC-tracers is a useful non-invasive method of investigating three-dimensional flow and temperature fields and their easy comparison with numerical results.

## References

1. W.J. Hiller, S. Koch, T.A. Kowalewski, and F. Stella, "Onset of natural convection in a cube", *Int. J. Heat Mass Transfer* **36**, 3251–3263 (1993).
2. T.A. Kowalewski and A. Cybulski, "Experimental and numerical investigations of natural convection in freezing water", *Int. Conf. on Heat Transfer with Change of Phase in Mechanics*, Kielce, Vol. 61, 7–16 (1996).
3. T.A. Kowalewski, A. Cybulski, and M. Rebow, "Particle image velocimetry and thermometry in freezing water", *8<sup>th</sup> Int. Symp. on Flow Visualisation, Sorrento*, edited by G.M. Carlomagno and I. Grant, CD ROM Proc, Edinburgh, 24.1–24.8 (1998).
4. T.A. Kowalewski and M. Rebow, "Freezing of water in the differentially heated cubic cavity", *Int. J. Comp. Fluid Dyn.* **11**, 193–210 (1999).
5. J. Stasiek and M.W. Collins, "The use of liquid crystals and true-colour image processing in heat and fluid flow experiments", *Atlas of Visualisation*, Vol. 2, CRC Press, Inc, 1996.
6. N. Akino, T. Kunugi, Y. Shiina, K. Ichimiya, and A. Kurosawa, "Fundamental study on visualisation of tempera-

- ture fields using thermosensitive liquid crystals”, in *Flow Visualisation V*, pp. 87-92, edited by R. Reznicek, Hemisphere Publishing Corp. Washington, 1990.
7. B&H Liquid Crystal Devices Ltd, London (1992).
  8. Data Translation Ltd: Image Processing Handbook (1991).
  9. J.W. Baughn and X. Yan, “Liquid crystal methods in experimental heat transfer”, *Proc. 32<sup>nd</sup> Heat Transfer and Fluid*, pp. 15–40, Mechanics Institute Sacramento, CA (1991).
  10. R.J. Moffat, “Describing the uncertainties in experimental results”, *Experimental Thermal and Fluid Sciences* **1**, 3–17 (1988).
  11. R.J. Moffat, “Experimental heat transfer”, *Proc. 9<sup>th</sup> Int. Heat Transfer Conference*, Jerusalem, Vol. 1, 308–310 (1991).
  12. T.V. Jones, Z. Wang, and P.T. Ireland, “The use of liquid crystals in aerodynamic and heat transfer experiments”, *Proc. 1<sup>st</sup> I. Mech. E. Seminar on optical methods and Data Processing in Heat and Fluid Flow*, City University, London, 51–65 (1992).
  13. S. Ashforth-Frost, L.S. Wang, K. Jambunathan, D.P. Graham, and J.M. Rhine, “Application of image processing to liquid crystal thermography”, *Proc. 1<sup>st</sup> I. Mech. E. Seminar on Optical Methods and Data Processing in Heat and Fluid Flow*, City University, London, 121–126 (1992).
  14. J. Stasiek, “Thermochromic liquid crystals and true colour image processing in heat transfer and fluid flow research”, *J. Heat Mass Transfer* **33**, 27–29 (1997).
  15. W. Leiner, K. Schulz, M. Behle, and S. Lorenz, “Imaging techniques to measure local heat and mass transfer”, *Proc. 3<sup>rd</sup> I. Mech. E. Seminar Optical Methods and Data Processing in Heat and Fluid Flow*, City University, London, 1–13 1996.